

A DIRECT PLASMA ETCH APPROACH TO HIGH ASPECT RATIO POLYMER MICROMACHINING WITH APPLICATIONS IN BIOMEMS AND CMOS-MEMS

Jeffrey D. Zahn^{1,3}, Kaigham J. Gabriel^{2,3} and Gary K. Fedder^{2,3}

1. Department of Bioengineering, Pennsylvania State University 2. The Robotics Institute, Carnegie Mellon University,
3. Department of Electrical and Computer Engineering, Carnegie Mellon University
224 Hallowell Building University Park, PA 16802 jdzbio@engr.psu.edu

ABSTRACT

A novel etching approach to high aspect ratio polymer micromachining is introduced. A switching chemistry utilizing oxygen as an etchant gas with a C_4F_8 passivation step has produced high aspect ratio polymer structures. Polymer layers have been bound to a mechanical silicon support, patterned and etched. The silicon is subsequently undercut creating suspended polymer membranes. The polymer microstructures have also been aligned with CMOS MEMS structures in a process compatible with post CMOS micromachining. All steps in the polymer micromachining and post CMOS release are compatible with standard MEMS processing equipment. This approach holds great promise for creating devices with CMOS electronics as sensors and actuators and aligned polymer microstructures serving as integrated fluidic conduits for bioMEMS and micro total analysis systems.

INTRODUCTION

Micromachined polymers are being increasingly utilized in the MEMS field, especially in microfluidic and bioMEMS applications. Much of the research has focused on fabricating structures using hot-embossing techniques [1], soft lithography [2] or laser micromachining [3]. However, these approaches generally produce independent components such as fluidic conduits. This makes device design more of a serial microassembly process than a parallel fabrication process, requiring the physical alignment of fluidic components with electromechanical actuators.

Lithographic techniques using polyimides or SU-8 photoresist [4] have also been employed. These approaches can produce aligned high aspect ratio polymer microstructures but lithographic approaches generally limit the number of materials that can be utilized.

A smaller amount of research has incorporated isotropic etching of thin parylene films [5], liquid crystal polymers [6] or ion-beam etching of fluoropolymers [7].

An alternative method using direct plasma etching of polymers with a Bosch-like switching chemistry to produce high aspect ratio structures is introduced. This approach is inspired by the deep reactive ion silicon etch [8,9], except oxygen is used as the etchant gas. Oxygen plasmas have long been used for polymer etching in processes such as photoresist ashing. The high energy oxygen molecules react with hydrocarbon (polymer) chains to produce carbon dioxide and water.

Switching between a directed oxygen etch step and an isotropic C_4F_8 fluoropolymer deposition step, produces high aspect ratio polymer structures. **This approach allows more densely packed devices with smaller minimum feature sizes than molding technology and the ability to integrate devices with underlying electronics.** It also increases the number of different polymers that may be micromachined.

Direct etch approaches allow mechanical structures to be layered on top of electronics. These structures may be simple fluidic conduits or could be an environmentally sensitive polymer film, which could change the response of a resonant actuator. The ability to pattern and etch polymer films allows more freedom in

MEMS design since the polymer can be chosen for its unique mechanical and chemical properties and not because of manufacturability due to chemical resistance.

FABRICATION

The deep plasma etching of polymers is obtained using a Surface Technology System (STS) inductively coupled plasma deep reactive ion etcher. During each passivation step, fluoropolymer is isotropically deposited across all exposed area of a wafer surface. After deposition the fluoropolymer is removed from the horizontal surface by reactive ion etching. RF biasing of the platen accelerates ions in the bulk plasma towards the horizontal surface of the wafer where they remove the passivation layer. These ions have high energy in the vertical direction, so the passivation layer is removed from the horizontal surface faster than the vertical direction. After the passivation layer is removed from the horizontal surface, the bulk material is exposed and etched by the reactive ions. Repeating the passivation and etching steps etches the material primarily in the vertical direction with suppressed lateral etching (undercut). In the standard silicon etch process, silicon is used as the bulk material with SF_6 as the etchant gas. In this study, a polymer is used as the bulk material with oxygen as the etchant gas.

Polymethylmethacrylate (PMMA) was chosen as a test material because of its long history in both the microelectronics industry (e.g. LIGA process, e-beam photoresist) and use in medical implants (e.g. bone cement). Since many polymers are reactive to, or soluble in the chemicals used during the fabrication process, a barrier film must be deposited onto the polymer surface to protect it (Fig. 1). First 1000-5000 Å of aluminum was evaporated onto the polymer as a barrier layer, patterned using Shipley 1813 positive photoresist with a Karl Suss MA56 mask aligner, and wet etched in aluminum etchant. Polymer etch recipes were then developed using the STS etcher. The critical processing variables were gas flow rates and the lengths of the oxygen etch and fluoropolymer passivation steps. The fabrication protocol and different etch recipes are summarized in Table 1.

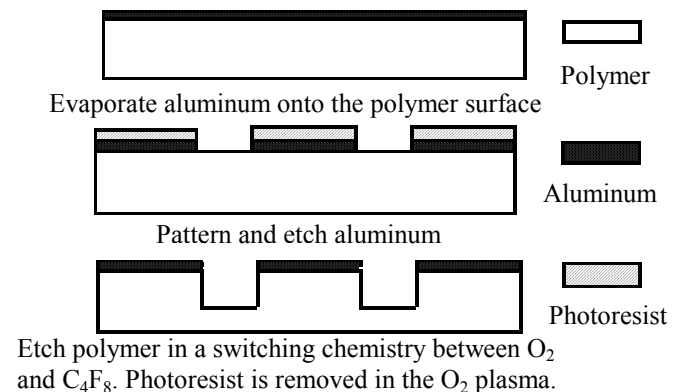


Figure 1. Process Flow for micromachining of polymer films.

Recipe	Isotropic Etch 1	Anisotropic Etch 1	Anisotropic Etch 2	Anisotropic Etch 3
O ₂ flow rate (sccm)	50	50	50	100
C ₄ F ₈ flow rate (sccm)	85	85	85	85
Etch Coil Power (W)	800	800	800	800
Etch Platen Power (W)	120	120	120	120
Passivation Coil Power (W)	NA	600	600	600
Passivation Platen Power (W)	NA	0	0	0
Etch time (sec)	NA	12	11	8
Passivation time (sec)	NA	8	9	7
Etch rate (μm/hr)	30	10	10	15
Aspect Ratio	3:1	5:1	10:1	20:1

Table 1 Polymer etch recipes developed

The second anisotropic etch recipe developed (Etch 2 in Table I) produced a 10:1 aspect ratio structure with an etch rate of 10 μm/hr (Fig. 2). In order to increase the etch rate and degree of anisotropy, the oxygen flow rate was increased while increasing the passivation time relative to the etch time. Fig. 3 demonstrates how tailoring recipes can increase the aspect ratio to 20:1 with an etch rate of 15 μm/hr (anisotropic etch 3).

In order to couple polymer structures to underlying electronics, a 50 μm thick PMMA film was bound onto a bare silicon wafer using PMMA photoresist (9% in chlorobenzene). The photoresist was spun onto the wafer surface at 500 RPM (Fig. 4). The bulk polymer film was placed onto the photoresist from the center radially outward to minimize trapped air bubbles. The photoresist was subsequently cured first at room temperature and then at 100 °C. The interdiffusion of the chlorobenzene into the bulk material promotes a strong bond between the bulk polymer and the photoresist. The polymer was then patterned, etched through the polymer layer and the underlying silicon was removed using a xenon difluoride (XeF₂) isotropic etch. This procedure undercut the film to create suspended polymer structures (Fig. 5).

In a slightly more complex process flow, the polymer film was patterned on top of a CMOS MEMS [10] chip. The modified CMOS-MEMS processing flow is shown in Figure 6. The CMOS passivation oxide was first etched in a CHF₃/O₂ (22.5:10 sccm 100 W) plasma using the CMOS aluminum metallization as a mask. Etching the oxide after polymer patterning destroys the polymer since the oxide etch also reacts with the aluminum mask from the top and the polymer substrate laterally. The polymer was

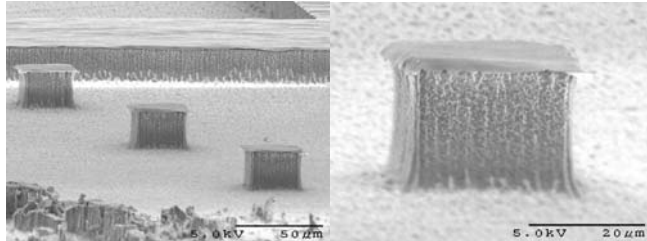


Figure 2. Typical results using Anisotropic etch recipe 2. (Left) A series of 20 X 20 μm² posts. (Right) Closeup of the center post.

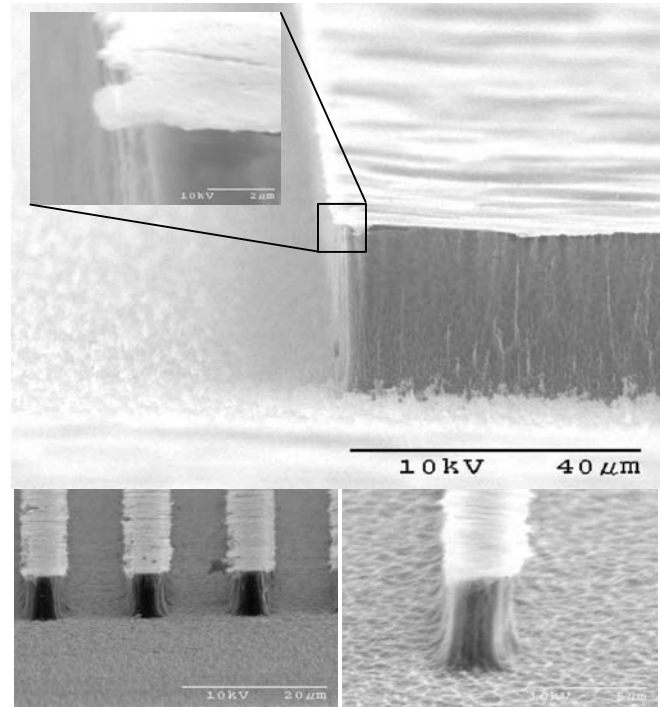


Figure 3. Typical results using Anisotropic Etch recipe 3. (Top) A sharp sidewall etched 30 μm into the substrate. The inset shows a closeup of the film showing less than 1 μm of undercut. (Bottom Left) A series of 5 μm lines. (Bottom right) A single 2.5 μm line

attached using PMMA resist, patterned and etched to stop on the surface of the CMOS chip. The microstructures were subsequently released in a XeF₂ etch. A series of test structures integrated with CMOS MEMS structures is shown in Fig. 7.

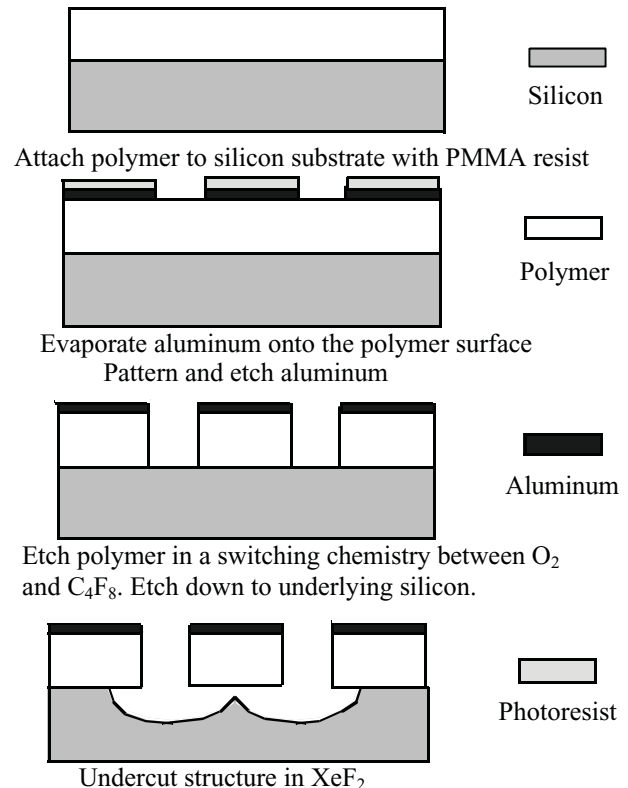


Figure 4. Process Flow for integrating a polymer film with an underlying silicon substrate.

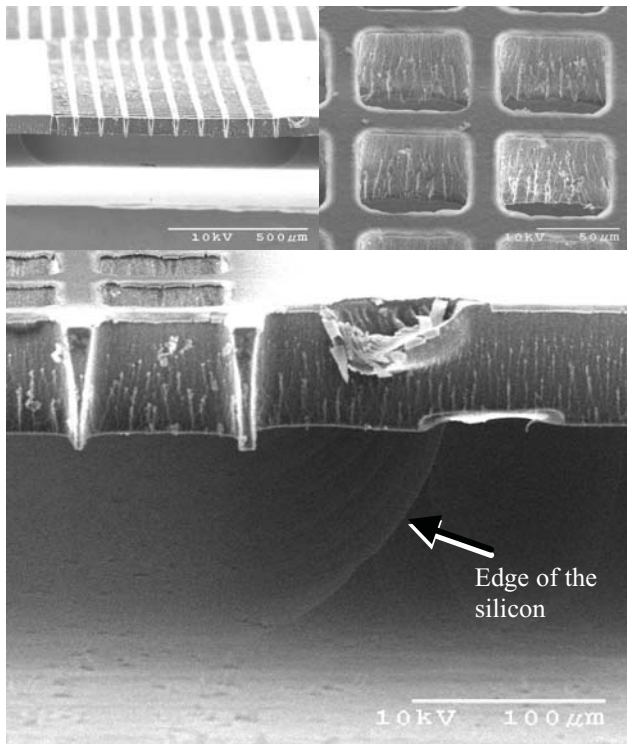


Figure 5. (Top Left) An etch polymer grid with the silicon undercut. (Top Right) An oblique top view of the grid. (Bottom) Closeup of the polymer membrane and undercut silicon. The bottom edge of the polymer shows some evidence of “footing” because of the etch stopping on the silicon substrate.

An acoustic membrane [11] has been previously produced in the CMOS MEMS process. By patterning polymer lines across the membrane surface (Fig. 8), it could be used as a diaphragm for microfluidic pumping with etched polymer microchannels for bio-MEMS applications. The polymer lines stiffened the membrane and separated the continuous membrane surface into subsections that actuate independently of each other. This work demonstrates an etch protocol which allows polymer integration with electronics which would be difficult to produce otherwise.

ISSUES IN POLYMER MICROMACHINING

Several issues were raised in the course of this study. First, the directional etch rate of the polymer film is appreciably slower than that of silicon. This is attributed to the more complex, multistep reactions that occur during combustion as opposed to silicon SF_6 chemistry. However, the etch rate for the isotropic polymer etch is similar to etch rates observed at similar conditions [6]. Second, the aluminum masking layer reacted with the fluorine based chemistry to produce particulates assumed to be aluminum fluoride evident in Fig 7. A more compatible masking material was investigated. ECR PECVD deposited silicon oxide and silicon nitride films were physically sputtered off the wafer surface in the oxygen plasma (data not shown). Further investigation into reducing aluminum fluoride particulates or a more appropriate masking layer is necessary. Third, the surface roughness and some evidence of “footing” of the polymer microstructures is apparent. The sidewall roughness and trench roughness is also thought to occur from aluminum fluoride deposition during etching. Also, the contact lithography and aluminum etching tolerance for small features was not well controlled. Better lithographic techniques

metallization layers
oxide
silicon substrate
circuitry

Etch oxide in a CHF_3/O_2 plasma using the top metallization layer of the CMOS chip as a mask. The CMOS circuitry is also depicted.

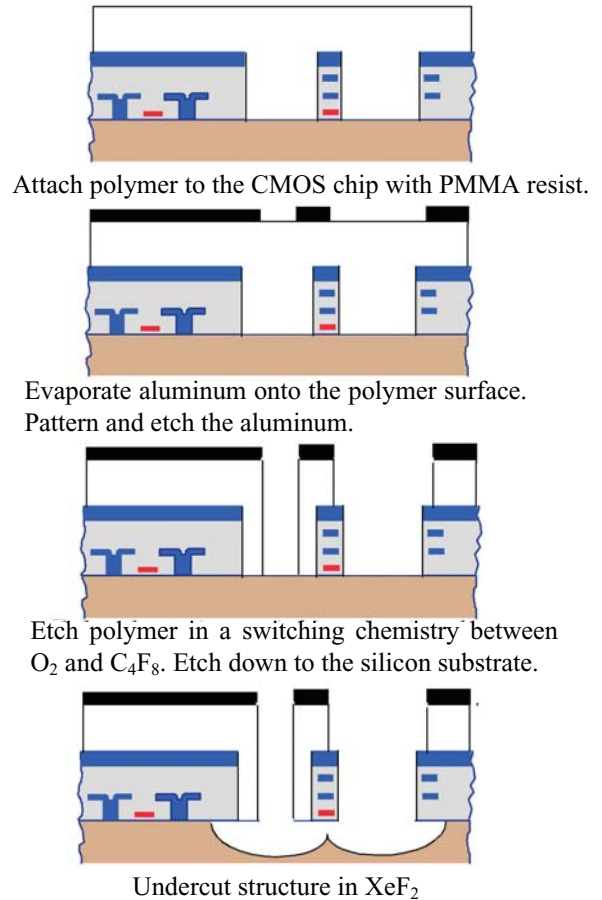


Figure 6. Process Flow for integrating a polymer film with CMOS MEMS structures.

(e.g. wafer stepper) with better small feature resolution and a plasma metal etch to produce better mask features may reduce sidewall roughness. Further recipe refinement will also attempt to reduce sidewall roughness and increase aspect ratio with longer passivation cycles.

Finally, polymers are highly sensitive to heat induced deformation. By increasing the cooling rate of the chuck, better feature protection may be achieved. The bonded polymer films had more reproducible results; presumably since the support silicon wafer is a better heat conductor to remove heat from the thin film, than the thicker bulk polymer.

CONCLUSIONS

A novel approach to polymer micromachining with integration to highly complex MEMS structures was demonstrated. This approach holds great promise to increasing the utilization of polymers in micromachining by allowing multilayer integrated systems to be produced with better coupling to electronic sensors and actuators.

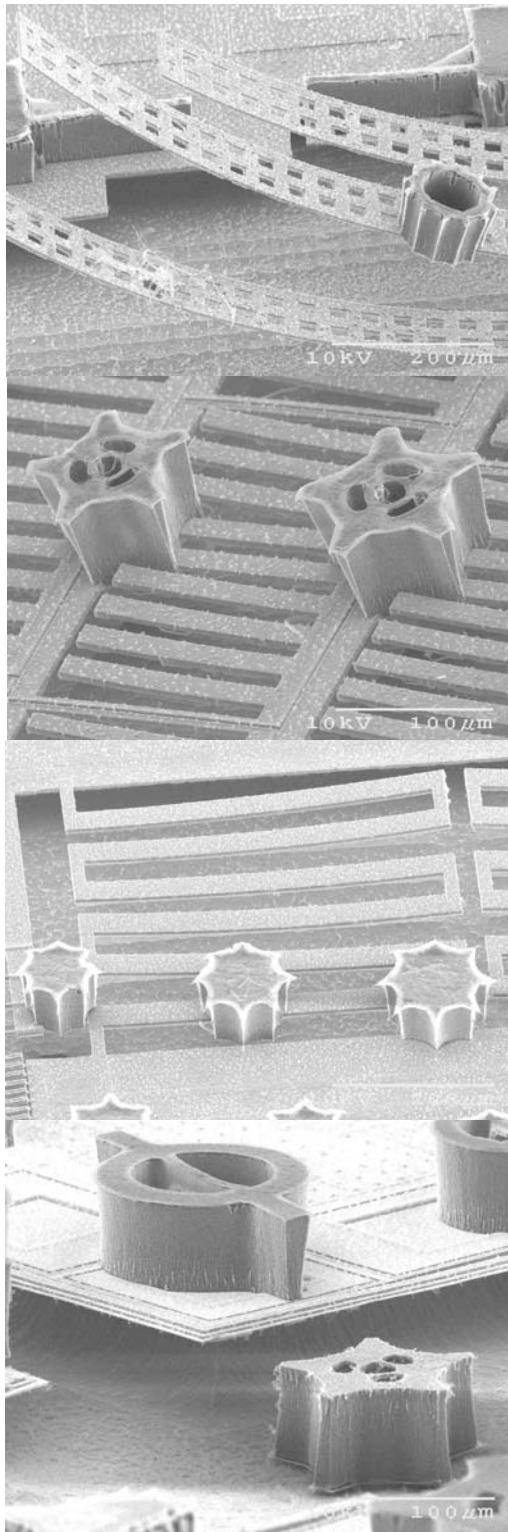


Figure 7. A series of shapes integrated with different CMOS MEMS structures. No bonding interface can be discerned between the PMMA photoresist and the bulk material. From the top: A MEMS plastic gear on a cilia beam structure. Two plastic pieces on a stress test structure. Gears sitting on a serpentine spring. Two shapes above and below an etched pit. The lower shape has fallen over into the pit after the supporting silicon was undercut.

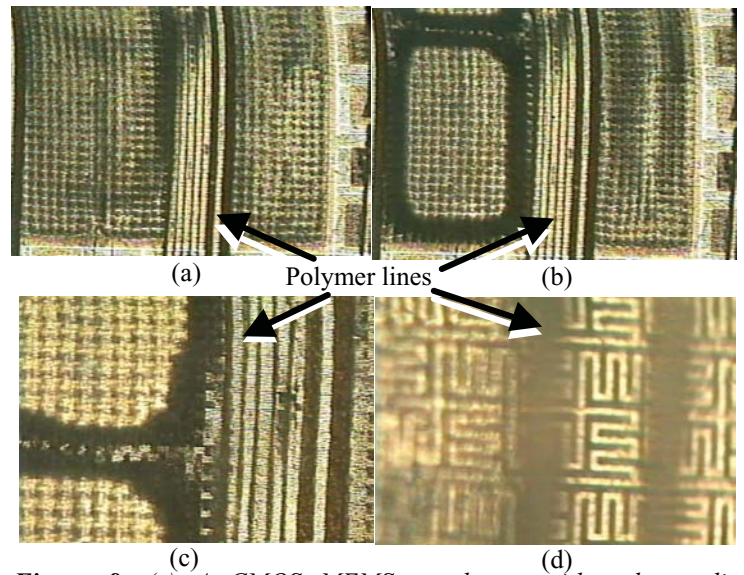


Figure 8. (a) A CMOS MEMS membrane with polymer lines patterned across it. (b) The membrane after being actuated (80 V bias) The membrane moves in two separate regions to the right and left of the patterned lines. The polymer lines do not move significantly since they are much stiffer. A mechanical node may be seen in the region to the left of the lines. (c) A closeup of the mechanical node. (d) A closeup of the membrane under the polymer lines. The serpentine mesh structure can be discerned.

ACKNOWLEDGEMENTS

The authors would like to thank Joe Suhan of the CMU Electron Microscopy Laboratory for SEM assistance and the members of the Fedder/Gabriel labs for technical discussions and assistance. This work was sponsored by a Keck Foundation grant (PI V. Weedn) and by DARPA under the AFRL, Air Force Materiel Command, USAF, under agreement F30602-97-2-0323.

REFERENCES

1. H. Becker and W. Dietz, "Microfluidic Devices for Micro-TAS Applications Fabricated by Polymer Hot Embossing," *SPIE Conference '98*, Santa Clara, CA, 1998.
2. Y. Xia, and G.M. Whitesides, "Soft Lithography," *Annu. Rev. Mater. Sci.*, V.28, pp: 153-184, 1998.
3. A. Schwarz, J. S. Rossier, F. Bianchi, F. Reymond, R. Ferrigno, and H. H. Girault, "Micro-tas On Polymer Substrates Micromachined by Laser Photoablation," in *Proceedings of the uTas '98 Work-shop*, pp. 241-244, 1998.
4. N. Kuan, D. Liepmann, and A.P. Pisano, "Fabrication and Packaging of Microfluidic Devices with SU-8 Epoxy," *Proceedings of the ASME MEMS 2000 Symposium*, Orlando Florida, November 5-10, pp: 591-594, 2000.
5. X.Q. Wang, Qiao. Lin and Y.C. Tai, "A Parylene Micro Check Valve," *Twelfth IEEE International Conference on Micro Electro Mechanical Systems (MEMS '99)*, Florida, USA, pp. 177-182, Jan. 17-21 (1999).
6. X. Wang, L.H. Lu and C. Liu, "Micromachining Techniques for Liquid Crystal Polymer," *Proceedings of the 14th IEEE International Conference on Micro Electro Mechanical Systems (MEMS '01)*, Interlaken, Switzerland, January 21-25, pp: 127-130, 2001.
7. L.P. Lee, S.A. Berger, D. Liepmann and L. Pruitt, "High Aspect Ratio Polymer Microstructures and Cantilevers for BioMEMS," *Sensors and Actuators A. Vol. A71/1-2*, pp. 144-149, 1998.
8. J. K. Bhardwaj and H. Ashraf, "Advanced Silicon Etching Using High Density Plasmas," *Proceedings of the Micromachining and Microfabrication Technology of the International SPIE*, Austin TX, October 23-24, V. 2639, pp: 224-233, 1995.
9. H. Ashraf, J.K. Bhardwaj, S. Hall, J. Hopkins, A.M. Hynes, I. Johnston, S. Mcauley, G. Nicholls, L. Atabo, M.E. Ryan and S. Watcham, "Advances in Deep Anisotropic Silicon Etch Processing for MEMS," *Proceedings of the 5th National Conference on Sensor and Microsystems*, The Italian Association of Sensors and Microsystems, Lecca Italy, Feb 14-16, 2000.
10. G. K. Fedder, S. Santhanam, M.L. Reed, S.C. Eagle, D.F. Guillou, M.S-C. Lu and L.R. Carley, "Laminated High-Aspect-Ratio Microstructures in a Conventional CMOS Process," *Sensor and Actuators A*, Vol. A57 pp:103-110, 1996.
11. J.J. Neumann and K.J. Gabriel, "CMOS-MEMS for Audio Frequency Acoustic Actuation," *Proceedings of the 14th IEEE International Conference on Micro Electro Mechanical Systems (MEMS '01)*, Interlaken, Switzerland, January 21-25, pp: 236-239, 2001.